DOI: 10.2478/cipms-2022-0029 Curr. Issues Pharm. Med. Sci., Vol. 35, No. 4, Pages 157-162

sciendo

Current Issues in Pharmacy and Medical Sciences

Formerly ANNALES UNIVERSITATIS MARIAE CURIE-SKLODOWSKA, SECTIO DDD, PHARMACIA

journal homepage: http://www.curipms.umlub.pl/



Features of the ultrastructure of the skin of white rats 30 days after modeling of portal hypertension

Nazar Hrytsevych[1*], Volodymyr Vereschaka[2]

[1] Department of Surgical Disciplines and Emergencies, Faculty No 2, Higher Educational Communal Institution of The Lviv Regional Council "Andrei Krupinsky Lviv Medical Academy", Lviv, Ukraine

[2] Department of Fundamental Medicine, Educational and Scientific Center "Institute of Biology and Medicine", Taras Shevchenko National University of Kyiv, Kyiv, Ukraine

ARTICLE INFO

Received: 07 June 2021
Accepted: 04 December 2022

Keywords:
portal hypertension,
ultrastructure of the skin,
electron microscopy.

ABSTRACT

The problem of skin repair under the conditions of systemic increased pressure in microvessels has a great importance. This is due to the fact that each year the incidence of this pathology has seen an increase during different operations, including plastic surgery. As the compensatory and reparative mechanisms occurring in the skin affected by vascular hyperbaria are still unidentified, the aim of the study was to investigate the features of the ultrastructure of the skin of white rats 30 days after modeling of portal hypertension. Objects of the study were anterior abdominal wall biopsies for electron microscopy research.

Our work demonstrated that the skin in intact animals (control group) was of typical structure before the beginning of the experiment and 30 days after a sham operation. Following 30 days modeling of portal hypertension, the ultrastructure of the epidermis was found to be intact, only slight thickening of the horny layer was revealed. However, in the basal epidermocytes, signs of crypts formation by cytolemma were revealed. Moreover, in the epidermocytes of the spinous and granular layers, the mitochondria, endoplasmic reticulum channels and ribosomes were almost non-evident. In addition, in the cytoplasm of the fibroblasts, a moderate amount of freely located ribosomes and a moderate number of polymorphic mitochondria were detected, while the lumens of the capillaries of the papillary layer of the dermis were narrowed. We also saw that the swelling of the cytoplasm in endothelial cells resulted in the narrowing of the microvessels lumen. What is more, the subendothelial zone was expanded – which is indicative of endothelial desquamation. Beyond the aforementioned, the nuclei of the endothelial cells were well contoured and had signs of chromatin condensation. Endothelial cells with signs of apoptosis were detected as well.

INTRODUCTION

The problem of skin repair under the conditions of systemic increased pressure in microvessels has great medical and scientific importance. This is due to the fact that, each year, the incidence of this pathology has been seen to increase during plastic surgery. The most common complication of facelift surgery, for example, is a hematoma [1-3]. This represents 0.2-8.0% of all complications of facelift operations, and complications in the form of hematomas were observed in 11% of all operations [4].

* **Corresponding author**
e-mail: hrytsevych@gmail.com

While the most common cause of hematoma is hypertension [5], another complication of facelift surgery is asymptomatic deep venous thromboses [6], and in this case, this complication is due to high blood pressure. Indeed, it is shown that in patients who are prepared for surgery, often the pressure increases in the preoperative and postoperative periods [7]. This state is defined as perioperative hypertension [8]. Its treatment reduces the frequency of hematoma formation in the postoperative period [9].

Another pathological condition that leads to changes in systemic blood flow, including that in skin vessels, is portal hypertension. Clinical signs of portal hypertension include signs of hyperdynamic circulatory state, such as jumping

© 2022 Author(s). This is an open access article distributed under the Creative Commons Attribution-NonComercial-No Derivs licence (http://creativecommons.org/licenses/by-nc-nd/3.0/)

pulse and tachycardia, as well as warm moist skin of the limbs and arterial hypotension [10,11].

Compensatory and reparative mechanisms occurring in the skin affected by vascular hyperbaria are not fully understood. In most of the articles, light microscopy was used, and it allowed elucidating the nature of degenerative, inflammatory and compensation and reparation processes. The involvement of tissue basophils, endothelial cells, fibroblasts, connective tissue and extracellular matrix in the development of the reparative process has not, however, been studied. Moreover, comparison of clinical manifestations with the data of electron microscopy remains an actual question, as well as its characteristics depending on the stage of the pathological process. The aim of the study was to investigate the features of the ultrastructure of the skin of white rats 30 days after modeling of portal hypertension.

MATERIALS AND METHODS

All experiments were carried out according to the European Council Directive on 24 November 1986 for Care and Use of Laboratory Animals (86/609/EEC) approved by the First National Congress for Bioethics (September 2001). Local approval was obtained from the the Ethical Committee of Educational and Scientific Center "Institute of Biology and Medicine", Taras Shevchenko National University of Kyiv, Kyiv, Ukraine.

The investigations were performed on 20 male white nonlinear rats aged 5 months, which were randomly divided into 2 groups of 10 animals in each. In the rats of the second group, portal hypertension was simulated by applying a ligature to the portal vein according to the conventional method [12]. After 30 days, under local anesthesia, anterior abdominal wall biopsies were taken. Material for electron microscopy research (20 skin bioptates, 10 in each group) were chopped into pieces up to 1 mm thick and fixed during 1.5-2 hours at 30°C with a three times change of osmic acid. After fixing, the slices were washed in 0.1 mol/L phosphate buffer, pH 7.4, dehydrated in increasing concentrations of ethanol, absolute acetone and propylene oxide, with preliminary postfixation and contrast induced through a saturated solution of uranyl acetate. The slices were then sealed in a mixture of epoxy and araldite. Afterwards, half-thin sections of 1 μm thickness were stained with a 1% solution of toluidine blue for light optical study and orientation of the selected area for the electron microscopic evaluation. Ultra-thin sections were subsequently prepared with the help of ultra-thinner "LKB" and studied using an electron microscope "Philips 400 T" at an accelerating voltage of 80 kV.

RESULTS

Electron microscopy showed that the skin in intact animals (I group) was of typical structure. The basement membrane of the epidermis was also most evident. In the cytoplasm of the basal epidermocytes, an average number of melanin granules, mitochondria, dense tonofibrils, ribosomes, individual tonofilaments, Golgi complex, endoplasmic reticulum channels were identified. Moreover, the nuclei had elongated shape, were quite evident, and contained nucleoli, chromatin granules located around the nuclear membrane (Fig. 1).



Electronogram 13,000×. Basal epidermocyte: in the cytoplasm, a moderate number of mitochondria, dense tonofibrils, ribosomes, individual tonofilaments, Golgi complex, endoplasmic reticulum channels are identifiable. The nuclear membrane is quite evident, while the nucleoplasma contains chromatin granules located around the cariolemma. The basement membrane of the epidermis is well marked

Figure 1. Skin of the anterior abdominal wall of a 5-month-old intact rat (control)

Our investigation also saw that the basal epidermocytes were tightly arranged, while in the spinous layer, many tonofibrils and desmosomes were detected. In addition, the granular layer was represented by keratohyalin granules of moderate density, and the horny scales displayed homogenized fibrillar material. Involutive desmosomes were identified in the contact places of the scales. The dermis fibroblasts were mostly spindle-shaped, and had a light elongated nucleus that contained 1-2 nucleoli. Their cytoplasm contained a substantial number of mitochondria with well-developed cristae, as well as a granular endoplasmic reticulum that occupied from 30% to 50% of the cytoplasm area (Fig. 2).



Electronogram 10,000×. Elongated fibroblasts with nuclei having equal distribution of chromatin are evident. Moreover, a significant number of endoplasmic reticulum channels are seen, on the surface of which a moderate number of ribosomes are located. In addition, lamellose complexes and well-structured mitochondria can be seen. In the dermis, longitudinally, transversally and slanting dicularly, sliced collagen fiber bundles are noticeable

Figure 2. Skin of the anterior abdominal wall of a 5-month-old intact rat (control)

The skin cells, structurally, contained vacuoles with narrow and moderately expanded profiles that held a fine-grained matrix, and 1-2 rows of ribosomes, attached to membranes. A well-defined lamellose complex was also identified. Tissue basophils of dermis were spherical, oval, fusiform, occurred individually and in small groups, and had a perivascular and perineural position that provided contact with endothelial cells and nerve endings. Their diameter varied from 3.4 to 15 microns. Depending on the shape of the nucleus, the basophils had a round or elongated shape, contained nucleoli, uniformly distributed chromatin and occupied about 8% of cell volume. The cytoplasm incorporated light and vacuolized granules, the thickness of the membrane of which was from 0.4 to 2 microns, that had a reticular electron-dense structure, and contained light and very light granules with a minimum amount of granular matter. The capillaries of the dermis had a normal structure, their walls were limited by 2-3 endothelial cells. The cytoplasm of these endothelial cells had an average density, and held a significant number of mitochondria, microfilaments, pinocitic vesicles along the luminal area of the nuclear membrane. The nuclei were elongated and well contoured, while the karyoplasm was represented by chromatin of medium density that was evenly distributed along the nucleoplasm. The pericytes had a characteristic structure and surrounded capillaries.

30 days after the beginning of the experiment, in rats wherein portal hypertension was simulated, the ultrastructure of the epidermis was intact, only slight thickening of the horny layer was revealed. The basement membrane of the epidermis was unevenly thickened to 100 nm, however, there were also areas of thinning. In the basal epidermocytes, signs of crypts formation by cytolemma were revealed. Moreover, homogenization of the cytoplasm was noted, as well as destruction of mitochondria and lysis, and violation of the integrity of the plasma membranes (Fig. 3).



Electronogram 22,000×. Within the basal epidermocyte, the cell membrane is preserved, tonofibrils are dense and thickened, while individual mitochondria are found as dark electron-dense structures with ruined crysts. The high density of the nucleus is mediated by polymorphous granules. The basement membrane of the epidermis is also unevenly thickened and homogenized

Figure 3. Skin of the anterior abdominal wall of a 6-month-old rat, 30 days after the start of the experiment (simulation of portal hypertension)

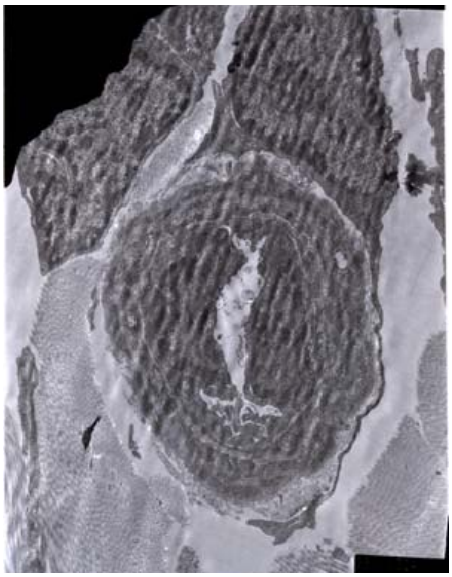
In their cytoplasm, tonofibrils and tonofilaments with a thickness of 4-8 nm were identified, which were uniformly distributed over the surface. Endoplasmic reticulum channels were also seen to be poorly contoured. The ribosomes were found to form groups of 3-8 units, and were of a small amount and scattered in the cytoplasm. The high density of the nucleus arose from the large number of highly packed polymorphic granules that resembled ribosomes. Many of these were especially noticeable in the zone of nuclear membrane. Signs of condensation and fragmentation of chromatin were also detected in the nucleus, and the chromatin were seen to be evenly distributed over the nucleoplasm. The nuclear membrane was gyrose, had small pores, was not visualized in certain areas. In the epidermocytes of the spinous and granular layers, the mitochondria, endoplasmic reticulum channels and ribosomes were almost non-evident, while the tonofibrils formed a network. In addition, a significant number of vacuoles and inclusions of different densities were detected in the cytoplasm. This was accompanied by the displacement of their nuclei to the periphery. They had many desmosomes and finger-like cytoplasmic growths. The grainy cells had a considerable density of cytoplasm due to the full development of the tonofibrils network and the high content of dense granules. Atypical granular cells with an increased electron density and a greater number of tonofibrils in the cytoplasm were found. Above the granular layer, several layers of horny scales were evident. These contained keratin and a significant number of vacuoles. Their significant rupture and desquamation were noted. The basement membrane of the epidermis, located between the basal layer of the epidermis and dermis, was unchanged, and had a thickness of 30 to 70 nm. Between the basement membrane of the epidermis and basal epidermis was a layer containing a transparent vacuole, the diameter of which did not exceed 50 nm. A layer of transversely, longitudinally and obliquely cut collagen fibrils approached this from the side of dermis. Bundles, as well as single fibrils with a thickness of 40-70 nm were clearly visualized in the dermis. Collagen fibrils were also unevenly distributed. Between their groups, transparent zones of irregular shape, arising due to edema, as well as swelling of the fibers and rupturing were revealed. Finally, the fibroblasts were bordered with collagen fibers (Fig. 4).

In the fibroblast cytoplasm, a moderate amount of freely located ribosomes were detected, while chains and ribosome clusters were noted, as well as channels of expanded granular endoplasmic reticulum (30-66 nm in diameter), on the membranes of which there was a small number of polymorphic ribosomes with a diameter of 5-10 nm. In the cytoplasm of the fibroblasts, there was a moderate number of polymorphic mitochondria (from 10 to 100 nm in diameter), most of which had signs of destruction and change in dimensional orientation. In contrast, the Golgi complex was of typical structure. However, near the cytolemma was a grouping of pinocytic vesicles of different diameters. Furthermore, the secretory vacuoles contained a substance of medium and low electron density. In addition, the cytoplasm of fibroblasts was dense, granular and deep, while the nuclei of the fibroblasts contained 1-2 nucleoli and condensed chromatin, which was distributed on islets in nucleoplasm. Around the



Electronogram 8,000×. The dermal fibroblasts show grouping of pinocytic vesicles of different diameters near the cytolemma. The secretory vacuoles are seen to contain a substance of medium and low electron density. Moreover, a moderate number of mitochondria with signs of destruction and changes of space orientation are noticeable. Myelin like structures within the cytoplasm are also evident

Figure 4. Skin of the anterior abdominal wall of a 6-month-old rat, 30 days after the start of the experiment (simulation of portal hypertension)



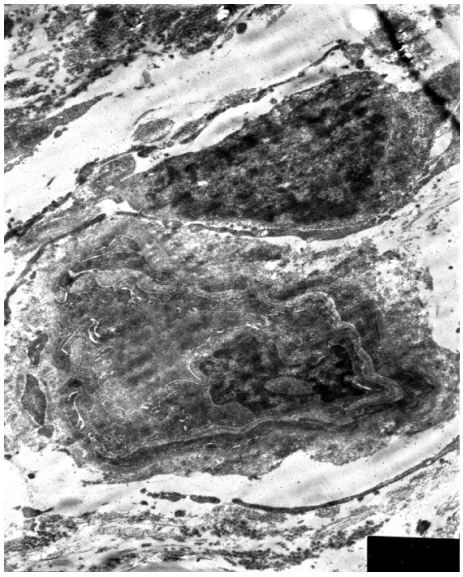
Electronogram 6,000×. Here, narrowing of microvessel lumen is noticeable, due to the edema of the cytolemma and endotheliocytes. On the luminal surface, the endotheliocytes cell membrane is well identified, as are gyrose and crypt forms. The loci of the cytoplasm display homogenization, while the subendothelial zone is expanded, indicating endothelium desquamation

Figure 5. Skin of the anterior abdominal wall of a 6-month-old rat, 30 days after the start of the experiment (simulation of portal hypertension)

fibroblasts, clusters of mature collagen fibers were identified that were tightly arranged. The lumens of the capillaries of the papillary layer of the dermis were narrowed (Fig. 5).

In the fibroblast cytoplasm, a moderate amount of freely located ribosomes were detected, while chains and ribosome clusters were noted, as well as channels of expanded granular endoplasmic reticulum (30-66 nm in diameter), on the membranes of which there was a small number of polymorphic ribosomes with a diameter of 5-10 nm. In the cytoplasm of the fibroblasts, there was a moderate number of polymorphic mitochondria (from 10 to 100 nm in diameter), most of which had signs of destruction and change in dimensional orientation. In contrast, the Golgi complex was of typical structure. However, near the cytolemma was a grouping of pinocytic vesicles of different diameters. Furthermore, the secretory vacuoles contained a substance of medium and low electron density. In addition, the cytoplasm of fibroblasts was dense, granular and deep, while the nuclei of the fibroblasts contained 1-2 nucleoli and condensed chromatin, which was distributed on islets in nucleoplasm. Around the fibroblasts, clusters of mature collagen fibers were identified that were tightly arranged. The lumens of the capillaries of the papillary layer of the dermis were narrowed (Fig. 5).

We noted that the endothelial cells had a moderately enlightened matrix, and individual hyperosmic cells were detected. In addition, spaces are identified in the places of their contacts, while swelling of the cytoplasm resulted in the narrowing of the microvessels lumen. What is more, the cell membrane in the luminal surface of the endothelial cell was well contoured, but was twisted and formed a crypt. In the cell cytoplasm, there was a moderate number of free ribosomes and an increased number of vacuoles along the luminal surface, while the mitochondria had signs of swelling and disorientation of cristae. Moreover, the endoplasmic reticulum was expanded, and homogenous loci of cytoplasm homogenization were identified. The subendothelial zone was also expanded, which is indicative of endothelial desquamation. Furthermore, the nuclei of the endothelial cells were well contoured, had signs of chromatin condensation, and endothelial cells with signs of apoptosis were detected, characterized by areas of the destroyed cell membrane, areas of cytolemma desquamation, destruction of mitochondria, lack of ribosomes, crypts and sharp winding of the basal and luminal surface of the cytolemma, as well as areas of a sharply enlightened cytoplasm. Finally, a significant number of polymorphic vacuoles were seen (Fig. 6).



Electronogram 6,000×. Endotheliocyte with apoptosis signs were noticeable, as well as the loci of destroyed cell membrane, foci of cytolemma detachment, mitochondria destruction, lack of ribosomes, crypts and sharp sinuosity of basal and luminal cytolemma surface areas of acutely enlightened cytoplasm

Figure 6. Skin of the anterior abdominal wall of a 6-month-old rat, 30 days following the start of the experiment (simulation of portal hypertension)

Electron microscopy indicated that their nuclear membrane lost its integrity, as chromatin was distributed over the cytoplasm. The precipitate was also scattered around the perivascular space, while the space between endothelial cells and pericytes was significantly enlarged. However, the cell and nuclear membrane of the pericytes were intact. Most tissue basophils had a reduced number of organoids, and isolated destructive mitochondria and polymorphic ribosomes in the perinuclear zone were seen, as well as poorly developed lamellosa complex and granular endoplasmic reticulum. In addition, a considerable number of microfilaments were detected in the cytoplasm, as were microtubules, crystalline bodies and lipid inclusions.

We noted that the tissue basophils that were located near microvessels, had higher functional activity, which was revealed by the granules released beyond the cytolemma. In the cytoplasm of the tissue basophils an increase of polymorphic transparent and dense granules content was evident, while the processes of degranulation were pronounced. In addition, the fibroblasts were elongated, and their nuclei occupied ⅔ of the cell volume, while the cytoplasm was presented by moderate granular endoplasmic reticulum, lamellose complex, lysosomes, mitochondria, phagosomes, pigment granules, vacuoles, polymorphic inclusions of various electron density. However, the elastic fibers were intact. In contrast, in free nerve endings, vacuolation and grainy disintegration of axial cylinders was observed. Still, correspondence of the collagen fibers direction according to the longitudinal axis of fibroblasts was preserved.

The use of experimental animal models to study the consequences of portal hypertension is of great importance, as they allow studying questions that cannot be resolved in human studies [13]. We employed the model of pre-hepatic portal hypertension [12]. Accordingly, already a week after applying a ligature to the portal vein, the rats develop portal hypertension with hyperdynamic circulation and portal-systemic shunting [14].

Utilizing the search terms „portal hypertension and wound healing in skin" in PubMed, we found only 2 papers [15,16]. At the same time, they are not related to the topic of our research. However, we found a lot of works devoted to cutaneous manifestations in disorders of hepatobiliary system. For example, Godara et al. stated: "The common mucocutaneous manifestations associated with primary hepatobiliary disorders were icterus, ichthyosis/xerosis, pallor, excoriations, hyperpigmented palmar creases, clubbing, and pedal edema" [17]. As for portal hypertension, it is known that collateral circulation develops against its background, including visible varicose veins on the abdominal wall ("caput Medusae") [18]. In the literature available to us, we did not find data on ultrastructural changes in the skin against the background of portal hypertension.

Previously, we showed that 60-90 days after simulation of portal hypertension in the skin of rats, ultrastructural changes of microvessels, which are characterized by narrowing of their lumen, develop [19]. Moreover, endothelial cells had significant edema. In this work, we established that already on the 30th day after simulation of portal hypertension, there is a narrowing of the lumen of microvessels due to swelling of the cytolemma and endotheliocytes. We also revealed the expansion of the subendothelial zone, which indicates desquamation of the endothelium. Such a state of hemomicrocirculation in the skin can be one of the reasons for both postoperative complications and prolongation of the healing time of the wound surface. The use of pharmacological drugs to improve microcirculation in patients with impaired microcirculation in the postoperative period will improve the results of surgical interventions and prevent the formation of thrombosis.

CONCLUSION

The use of electron microscopy allowed us to found the features of the ultrastructure of the skin of rats 30 days after modeling of portal hypertension. In our work, we noted:

1. In basal epidermocyte, the tonofibris were dense, thickened. High density of the nucleus was mediated by polymorphous granules. The basement membrane of the epidermis was unevenly thickened and homogenized.
2. In the dermal fibroblasts, we found grouping of pinocytic vesicles of different diameters near the cytolemma. There were a moderate number of mitochondria with signs of destruction and changes of space orientation.
3. Narrowing of microvessels lumen was seen, given the edema of cytolemma and endotheliocytes. The subendothelial zone was expanded, indicating endothelium desquamation.
4. Endotheliocytes were with apoptosis signs, among others, the loci of destroyed cell membrane, foci of cytolemma detachment, mitochondria destruction, lack of ribosomes, crypts and sharp sinuosity of basal and luminal cytolemma surface areas of the acutely enlightened cytoplasm.

CONFLICT OF INTEREST

The authors declare that there is no conflict of interest. All authors have equally contributed to the above work.

ETHICAL APPROVAL

The Ethical Committee of Educational and Scientific Center "Institute of Biology and Medicine", Taras Shevchenko National University of Kyiv, Kyiv, Ukraine.

ORCID iDs

Nazar Hrytsevych https://orcid.org/0000-0002-9627-2099
Volodymyr Vereschaka https://orcid.org/0000-0003-0978-8028

REFERNCES

1. Maricevich MA, Adair MJ, Maricevich RL, Kashyap R, Jacobson SR. Facelift complications related to median and peak blood pressure evaluation. *Aesthetic Plast Surg.* 2014;38(4):641-7.
2. Park DM. Total facelift: Forehead lift, midface lift, and neck lift. *Arch Plast Surg.* 2015;42(2):111-25.
3. Cason RW, Avashia YJ, Shammas RL, Savetsky IL, Rohrich RJ. Perioperative approach to reducing hematoma during rhytidectomy: What does the evidence show? *Plast Reconstr Surg.* 2021;147(6):1297-309.

4. Swanson E. Evaluation of face lift skin perfusion and epinephtine effect using laser fluorescence imaging. *Plast Reconstr Surg Glob Open*. 2015;3(8):e484.
5. Baker DC, Stefani WA, Chiu ES. Reducing the incidence of hematoma requiring surgical evacuation following male rhytidectomy: A 30-year review of 985 cases. *Plast Reconstr Surg.* 2005;116(7):1973-85.
6. Swanson E. Prospective study of Doppler ultrasound surveillance for deep venous thromboses in 1000 plastic surgery outpatients. *Plast Reconstr Surg.* 2020;145:85-96.
7. Varon J, Marik PE. Perioperative hypertension management. *Vasc Health Risk Manag.* 2008;4(3):615-27.
8. Chung KH, Cho MS, Jin H. Perioperative hypertension management during facelift under local anesthesia with intravenous hypnotics. *Arch Plast Surg.* 2017;44(4):276-82.
9. Trussler AP, Hatef DA, Rohrich RJ. Management of hypertension in the facelift patient: results of a national consensus survey. *Aesthet Surg J.* 2011;31:493-500.
10. Conn HO. Portal hypertension, varices and transjugular intrahepatic portosystemic shunts. *Clin Liver Dis.* 2000;4(1):133-50.
11. Gunarathne LS, Rajapaksha H., Shackel N, Angus PW, Herath CB. Cirrhotic portal hypertension: from pathophysiology to novel therapeutics. *World J Gastroenterol.* 2020;26(40):6111-40.
12. Königshofer P, Brusilovskaya K, Schwabl P, Reiberger T. Animal models of portal hypertension. *Biochim Biophys Acta Mol Basis Dis.* 2019;1865(5):1019-30.
13. Abraldes JG, Pasarin M, Garcia-Pagan JC. Animal model of portal hypertension. *World J Gastroenterol*. 2006;12(41):6577-84.
14. Sikuler E, Kravetz D, Groszmann RJ. Evolution of portal hypertension and mechanisms involved in its maintenance in a rat model. *Am J Physiol.* 1985;248:G618-G25.
15. Zhu W, Song H. A rare case of recurrent lower extremity ulcer. *Int J Low Extrem Wounds*. 2019;18(4):389-92.
16. Van Buuren HR, Fick TE, Schalm SW. Recurrent bleeding from cutaneous venous collaterals in portal hypertension. *Gut*. 1988;29(9):1279-81.
17. Godara SK, Thappa DM, Pottakkatt B, Hamide A, Barath J, Munisamy M, et al. Cutaneous manifestations in disorders of hepatobiliary system. *Indian Dermatol J Online*. 2017;8(1):9-15.
18. Sato I. Cutaneous manifestations of liver cirrhosis. *Nihon Rinsho*. 1994;52(1):170-3.
19. Hrytsevych NR, Vereschaka VV. Features of the ultrastructure of the skin of white rats 60 and 90 days after modeling of portal hypertension. *Wiad Lek*. 2021;74(9 part 1):2197-201.